

# Thermal and crystallization studies of nano-hydroxyapatite reinforced polyamide 66 biocomposites

Xiang Zhang, Yubao Li\*, Guoyu Lv, Yi Zuo, Yuanhua Mu

*The Research Centre for Nano-Biomaterials, Institute of Materials Science and Technology, 4th floor, Analytical & Testing Center, Sichuan University, Chengdu 610064, PR China*

Received 21 December 2004; received in revised form 6 February 2005; accepted 8 February 2005  
Available online 9 December 2005

## Abstract

The thermal and crystalline behaviour of nano-hydroxyapatite (n-HA) reinforced polyamide 66 (PA66) biocomposites was studied by thermogravimetry (TG) and differential scanning calorimetry (DSC). The thermal properties of PA66 and n-HA/PA66 composites were analysed by TG. The effect of hydroxyapatite on the melting and crystallization of PA66 was evaluated by DSC. DSC measurements exhibited an increase in the crystallization temperature, however, decrease in crystallinity with the addition of n-HA to the PA66 matrix, which was attributed to the hydrogen bonds between the n-HA surface and polyamide 66 molecules. With increase of n-HA content, the melting peak of the PA66 component shifted to higher temperature, suggesting constrained melting. The addition of n-HA to PA66 played the role of nucleating agent and enhanced the crystallization rate. Non-isothermal parameter  $\alpha$  measured by Liu method varies from 1.13 to 1.18, from 1.02 to 1.07, and from 1.18 to 1.21 for PA66, 30 wt% n-HA/PA66 and 40 wt% n-HA/PA66, respectively, and the values of  $K_{(T)}$  systematically increase with rise in relative degree of crystallinity. © 2005 Elsevier Ltd. All rights reserved.

**Keywords:** Thermal analysis; Crystallization; Nano-hydroxyapatite; Polyamide 66; Biocomposite

## 1. Introduction

Hydroxyapatite (HA,  $\text{Ca}_{10}(\text{PO}_4)_6(\text{OH})_2$ ) has been used for orthopaedic/dental implants because of its similar chemical composition and structure to the mineral phase of human bone, and it can promote sufficient new bone formation for the firm attachment of juxtaposed bone. However, due to low fracture toughness, HA cannot serve as a bulk implant material under high physiological loading conditions. Therefore, development of biocomposites with good mechanical properties, excellent bioactivity and biocompatibility similar to natural bone to meet the need of hard tissue repair has been a hot topic for over 30 years. To obtain

an advanced mechanical performance of the bioactive composite, bioceramic particles were usually incorporated into the polymer matrix using conventional plastics processing technology [1–8].

n-HA/PA66 biocomposites for load bearing bone repair were first prepared by a group led by Yubao Li and coworkers [9–11]. In the composite, n-HA nano crystals can keep their nano grade dispersion in the PA66 matrix and the content of n-HA can reach 65 wt%. The bending strength, tensile strength and compressive strength of the composite with 64.25 wt% n-HA are 95, 79 and 117 MPa, respectively, which are close to natural bone (80–100, 60–120, 50–140 MPa, respectively [12]), and the elastic modulus of this composite is 5.6 GPa. However, the elastic modulus of bioceramics and medical metals is much higher (70–300 GPa) than that of the natural bone (3–25 GPa) and this often causes stress stimulation or shielding effect,

\* Corresponding author. Tel./fax: +86 28 8541 7273.  
E-mail address: [nic7504@scu.edu.cn](mailto:nic7504@scu.edu.cn) (Y. Li).

resulting in bone resorption and loosening of implants [13,14]. Therefore, the mechanical properties of n-HA/PA66 composite can match well to that of human bone. Animal and clinical experiments have proved that the composite has good compatibility to bone and can bond to bone directly.

Thermal analysis is an important analytical method in understanding the structure–property relationships and mastering the technology for molecular design and industrial production of different polymeric materials, especially inorganic reinforced polymeric composites. Moreover, it is a useful technique to determine the thermal stability of the materials. In addition, it is possible to quantify the amount of moisture and volatiles present, which will weaken the physical and chemical property of composites. One of the accepted methods for studying the thermal property of polymeric materials is thermogravimetry (TG). Thermogravimetric data indicate a number of stages of thermal breakdown, weight loss of the material in each stage, threshold temperature, etc. [15]. Both TG and derivative thermogravimetry (DTG) will provide information about the nature and extent of degradation of the material. In differential scanning calorimetry (DSC), the heat flow rate associated with a thermal event can be measured as a function of time and temperature allowing one to obtain quantitative information about melting and phase transitions of the composite system.

The chemical and physical properties of polymer materials and polymeric matrix composites are mainly influenced by their thermal stability and crystallization behaviour. Thermal analysis studies of polyamide layered silicate nanocomposites (PLSN) have been carried out extensively [16–18]. Till now, no study has been made on the thermal and crystallization behaviour of n-HA/PA66 biocomposites. The aim of this work is to study the crystallization and thermal behaviour of n-HA reinforced polyamide 66 biocomposites, by means of TG, DTG and DSC.

## 2. Experimental

### 2.1. Materials

Polyamide 66 (PA66) with a viscosity-average molecular weight ( $M_v$ ) of 18 kDa was from BASF, Germany. The slurry of nano-hydroxyapatite (n-HA) crystals used for compounding was prepared by our laboratory.

### 2.2. Preparation of n-HA/PA66 composites

The preparation of n-HA/PA66 composites was given in Ref. [11]. The slurry of n-HA was added in *N,N*-dimethyl acetamide (DMAc) by stirring at the

temperature of 140 °C, then PA66 was added into the solution, keeping the temperature at 140 °C for 4 h till PA66 was dissolved completely. When the reaction ended, the co-precipitation mixture was set for 24 h at room temperature, then fully washed by deionized water and ethanol. The obtained n-HA/PA66 composite was dried in a vacuum oven at 80 °C for 48 h.

Samples of pure PA66 and n-HA/PA66 for TG and DSC measurements were ground into powder.

### 2.3. Thermogravimetric analysis

TG and DTG were carried out using PE DT-40 instrument, in a nitrogen atmosphere at a heating rate of 10 °C/min. Samples used for testing contained 9–10 mg of material. The scanning temperature scope was from 20–800 °C. The samples of polyamide 66 with and without n-HA were heated at 80 °C for 72 h to eliminate the humidity of the samples.

### 2.4. Crystallization behaviour analysis

The melting and crystallization behaviour of n-HA/PA66 composites was studied using a Netzsch-Phoenix differential scanning calorimeter (DSC) in a nitrogen atmosphere. The melting samples were kept at 290 °C for 5 min to eliminate heating history before cooling. Samples for testing contained about 10 mg of material. Again, the samples of polyamide 66 with and without n-HA were heated at 80 °C for 72 h to eliminate the humidity of the samples.

## 3. Results and discussion

### 3.1. Thermogravimetric analysis

Thermogravimetric curves of n-HA, PA66 and n-HA/PA66 composites containing 35 wt% n-HA are shown in Fig. 1. The temperature range used for the analysis is 20–800 °C. For HA (Fig. 2), dehydration occurs in the whole temperature range of 35–800 °C and most of the water is vaporized in the temperature range of 145–620 °C. PA66 starts to decompose at a temperature of 361 °C. Fig. 1 reveals that n-HA/PA66 degrades at higher temperature than does the PA66, i.e. the thermal stability of the composite is higher. The increased stability of the composite compared to PA66 may result from the hydrogen bonds between n-HA and PA66 matrix, which strengthens the interfacial action between PA66 macromolecules [11]. Fig. 2 shows that TG curve of n-HA can be divided into three stages. Stage 1 (35–145 °C) corresponds to the vaporization of adsorbed water on the surface of n-HA, stage 2 (145–620 °C) is due to the vaporization of the water of crystallization of hydroxyapatite, and stage 3 (620–800 °C) is probably

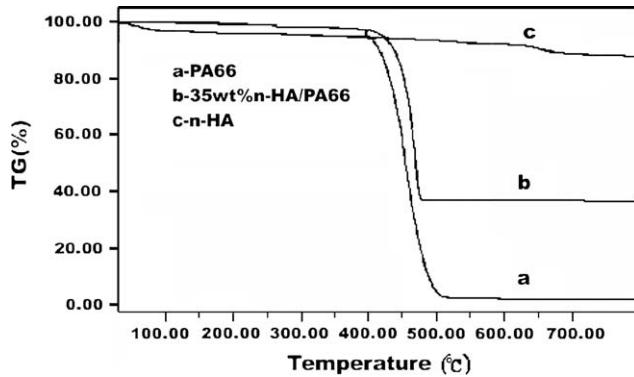


Fig. 1. The TG curves of PA66 (a), 35 wt% n-HA/PA66 (b) and n-HA (c).

due to the breakage of  $\text{CO}_3^{2-}$  and  $\text{HPO}_4^-$  in n-HA [19]. Fig. 3 shows the effect of n-HA content on thermal stability of n-HA/PA66 composites. It is found from Fig. 3 that the thermal stability of the composites is improved with the increase of n-HA content, however, the temperature range of degradation becomes narrower. DTG curves also give the same evidence (Fig. 4). From Fig. 4, it is clear that the peaks in the case of n-HA/PA66 composites are shifted to higher temperature compared to those of PA66, suggesting that the thermal stability of the composites is higher than that of pure PA66 due to n-HA–PA66 matrix interactions. The thermal parameters obtained from TG and DTG curves are given in Table 1. This is associated with the interactions between hydroxyapatite and PA66 matrix, due to the formation of hydrogen bonds between the amide group ( $-\text{NH}-\text{C}=\text{O}$ ) of PA66 and hydroxyl group ( $-\text{OH}$ ) of n-HA [9–11]. The possible chemical structures of hydroxyapatite–polyamide 66 are given in Fig. 5.

### 3.2. Differential scanning calorimetry (DSC) studies

#### 3.2.1. The melting behaviour of PA66 and n-HA/PA66

Fig. 6 shows the curves for the melting of PA66 and n-HA/PA66 composites. The DSC curve of PA66 shows

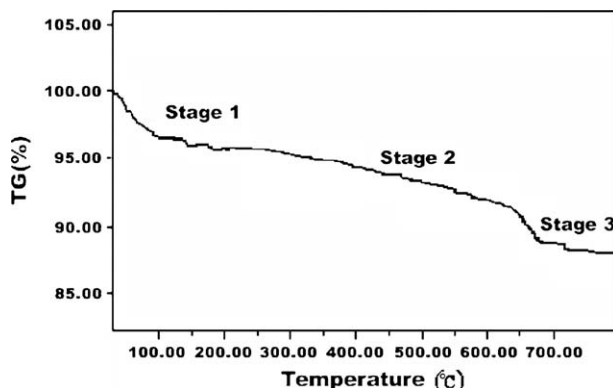


Fig. 2. The TG curve of n-HA.

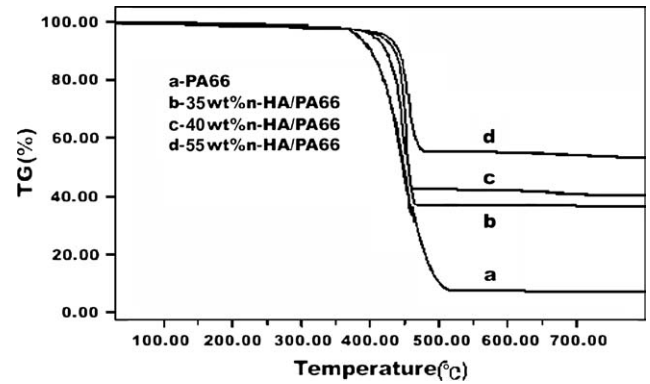


Fig. 3. The effect of n-HA on TG curves for n-HA/PA66 bio-composites.

two melting peaks with peak maximum temperature at 232 °C and 265 °C, respectively, however, the n-HA/PA66 composites show only one melting peak. The first melting peak of PA66 corresponds to its Brill transition due to the movement between the crystal sheets in PA66 [20]. For n-HA/PA66 composites, no Brill transitions are observed, probably because the interactions between PA66 molecules and n-HA particles will block the movement of PA66 crystal sheets.

Fig. 7 shows the DSC curves for the crystallization behaviour of PA66 and n-HA/PA66 composites with different content of n-HA at a cooling rate of 10 °C min. The values of the temperature for initial crystallization ( $T_{ci}$ ), temperature for maximum crystallization ( $T_{c,max}$ ), time for half crystallization ( $t_{1/2}$ ), heat for crystallization ( $\Delta H_c$ ) and the degree of crystallization ( $X_c$ ) of PA66 and n-HA/PA66 composites are listed in Table 2. The degree of crystallization of the PA66 component was determined by using the following relationship:

$$X_c \% = \Delta H_c \times 100 / \Delta H_c^0 \quad (1)$$

where  $X_c$ —degree of crystallization of PA66 component,  $\Delta H_c^0$ —heat of crystallization for 100% crystalline PA66, which is 188 J/g [21],  $\Delta H_c$ —heat of crystallization for PA66 and n-HA/PA66 composites.

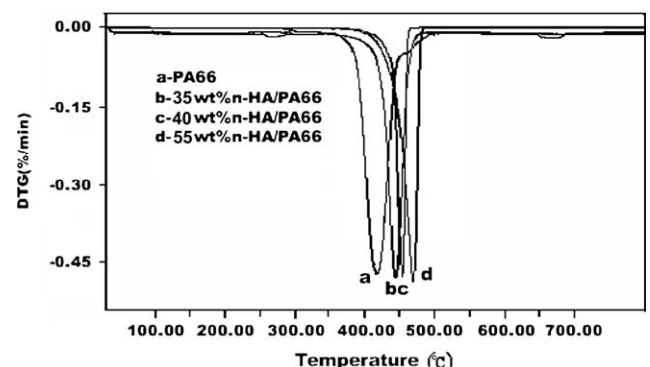


Fig. 4. The DTG curves of PA66 and its composites.

Table 1  
Thermal properties of PA66 and n-HA/PA66 composites from TG and DTG curves

n-HA/PA66 (wt%)	$T_i$ (°C)	$T_f$ (°C)	$\Delta T = T_f - T_i$ (°C)	$T_{max}$ (°C)
0/100	351	502	151	424
35/65	369	482	113	432
40/60	375	476	101	448
55/45	378	468	90	452

It clearly shows from Table 2 that: (1)  $T_{ci}$  and  $T_{c,max}$  of the composites are 5–6 °C and 9–10 °C higher than those of PA66, respectively. This is because the hydrogen bonds between PA66 and n-HA limit the rearrangement of PA66 molecules, resulting in the increase of the crystallinity temperature of PA66 in composites; (2) with the increase of n-HA in composites, the degree of crystallization of PA66 decreases, indicating that the addition of n-HA to PA66 matrix weakens the crystallizing capacity of PA66, because increasing the content of n-HA in the PA66 matrix will enhance the melt viscosity of composites, and the higher the melt viscosity, the harder it is for the PA66 macromolecules to rearrange regularly to form crystals. (3)  $t_{1/2}$  of PA66 is higher than those of composites, i.e. the crystallizing rate of the former is slower than those of the latter. The reason is that n-HA crystals in PA66 play a role as nucleating agents and enhance the crystallization growth rate. However, the ratio of n-HA in the composites has little effect on the crystallizing rate of PA66 component in the composites.

### 3.2.2. Non-isothermal crystallization behaviour of PA66 and n-HA/PA66 composites

Non-isothermal crystallization studies were carried out by heating to 280 °C and holding for 5 min prior to cooling. Figs. 8–10 compares DSC cooling curves for PA66 and n-HA/PA66 composites at different cooling rate. The composites have higher crystallization temperature and narrower peak width than PA66 at the same cooling rate. The higher crystallization temperature results from the increased crystallization rate arising from thermal and stress histories that remain after melting. Evidence of such effects has been reported by Khanna et al. [22–25] and Aharoni [26]. The crystallization temperature increased with the n-HA content, indicating some destruction of stable crystallites. However, introducing too many n-HA crystals to

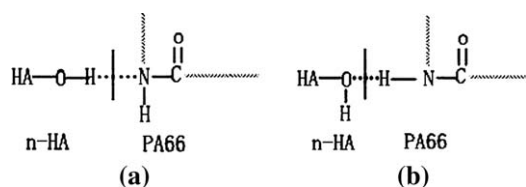


Fig. 5. The patterns of hydrogen bonds between n-HA and PA66.

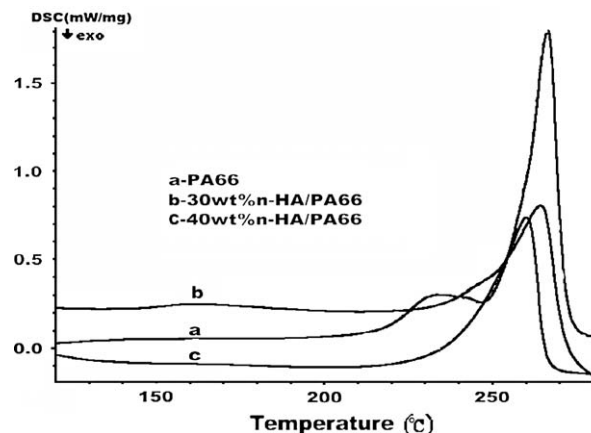


Fig. 6. The DSC curves of PA66, 30 wt% n-HA/PA66 and 40 wt% n-HA/PA66 at the heating rate of 10 °C/min.

PA66 matrix will hinder chains mobility of PA66 macromolecules and, thus, retard crystal growth resulting in decreasing of degree of crystallization.

Various non-isothermal crystallization kinetic models [29,30] have been developed based on the Avrami equation [27]. The Avrami equation is an isothermal model used universally to describe polymer crystallization kinetics. The change in crystallinity with time can be expressed as:

$$X_c = 1 - \exp(kt^n) \quad (2)$$

where  $X_c$  is the relative crystallinity at time  $t$ ;  $n$ , the Avrami index (crystal geometry information); and  $k$ , the isothermal crystallization rate constant containing the nucleation and growth rates. Eq. (2) can be transformed into logarithmic form:

$$\log[-\ln(1 - X_c)] = \log k + n \log t \quad (3)$$

However, in many cases, isothermal models are experimentally accessible only over a narrow temperature range that is often well above that where crystallization

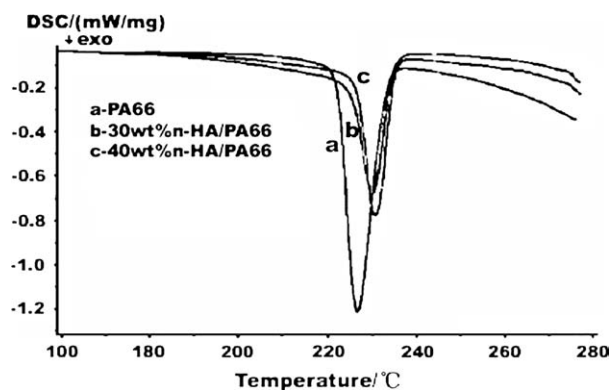


Fig. 7. DSC curves of PA66 and n-HA/PA66 composites at the cooling rate of 10 °C/min.

Table 2  
Thermodynamic parameters of polyamide 66 and its composites

Samples	$T_{ci}$ (°C)	$T_{c,max}$ (°C)	$t_{1/2}$ (min)	$\Delta H_c$ (J/g)	$X_c$ (%)
n-HA/PA66					
PA66	232	225	0.60	52.02	27.67
30 wt% n-HA/PA66	238	235	0.54	44.07	23.44
40 wt% n-HA/PA66	237	234	0.53	43.10	22.92

occurs in processing [28]. Non-isothermal modelling is therefore essential for the understanding of the crystallization behaviour of a semicrystalline polymer.

Ozawa [29] derived a non-isothermal kinetics model for the process of nucleation and its growth by extending the Avrami equation. The kinetic analysis of the thermoanalytical data of the process was applied to DSC curves of crystallization obtained by cooling the melt at constant rates. The following equation was proposed:

$$\log[-\ln(1 - X_c)] = \log K_{(T)} + m \log R \quad (4)$$

where  $K_{(T)}$  is the cooling function for non-isothermal crystallization at temperature  $T$ ,  $R$  is the cooling rate and  $m$  is the Ozawa exponent depending on the dimension of the crystal growth. Actually, Ozawa's equation has little application in process modelling because a constant cooling rate is assumed and values of relative crystallinities at a fixed temperature for different cooling rates are required. Furthermore, the theory and method of analysing thermoanalytical curves for the process of nucleation and growth described by Ozawa neglect the secondary crystallization that follows primary crystallization.

Considering the shortcomings of Ozawa and Avrami equations, Liu et al. [30] built another model by rearrangement at a given crystallinity  $X_c$  on the basis of Ozawa and Avrami equations for non-isothermal kinetics as follows:

$$\log R = \log F_{(T)} - a \log t \quad (5)$$

where  $F_{(T)} = [K_{(T)}/k]^{1/m}$  refers to the value of cooling rate, which must be chosen within unit crystallization

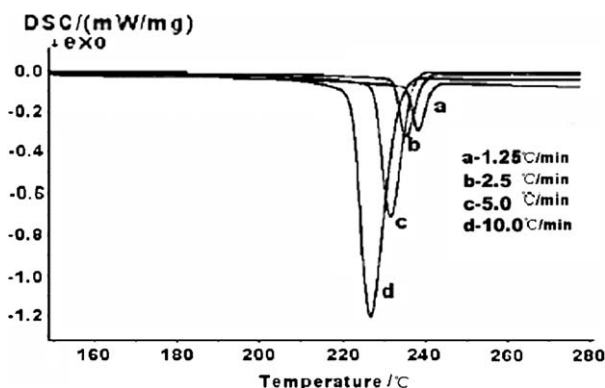


Fig. 8. DSC curves of PA 66 at different cooling rates.

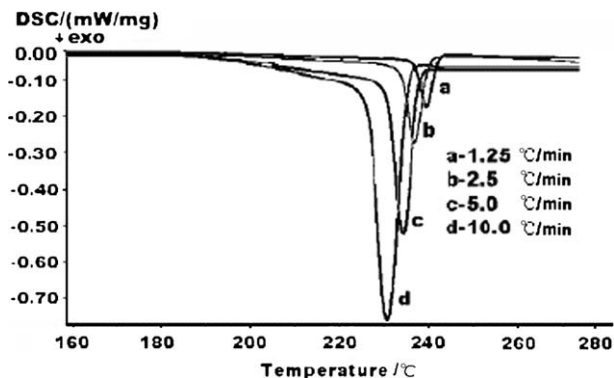


Fig. 9. DSC curves of 30 wt% n-HA/PA66 composites at different cooling rates.

time when the measured system has to a certain degree of crystallinity,  $a = n/m$ , the ratio of Avrami index  $n$  to Ozawa index  $m$ . According to Eq. (5), at a given degree of crystallinity, plotting  $\log R$  vs.  $\log t$  (Fig. 11) yields a linear relationship between  $\log R$  and  $\log t$ . The kinetic parameters  $K_{(T)}$  and  $a$  determined from the intercept and slope of the lines are listed in Table 3 for PA66 and n-HA/PA66 composites. It can be seen from Table 3 that the value of  $a$  for PA66 varies from 1.13 to 1.18, from 1.02 to 1.07 for 30 wt% n-HA/PA66 and from 1.18 to 1.21 for 40 wt% n-HA/PA66, and that the values of  $K_{(T)}$  systematically increase with the relative degree of crystallinity. It is also obvious that for a certain relative degree of crystallinity, the value of  $K_{(T)}$  for n-HA/PA66 is smaller than that for PA66, that is, amounting to same relative degree of crystallinity, n-HA/PA66 requires smaller cooling rate, which indicate that n-HA/PA66 crystallizes at a quicker rate than PA66. Obviously this approach is successful in describing the non-isothermal process of PA66 and n-HA/PA66 composites.

#### 4. Conclusions

TGA and DSC analytical measurements were carried out to study the thermal and crystallization behaviour of

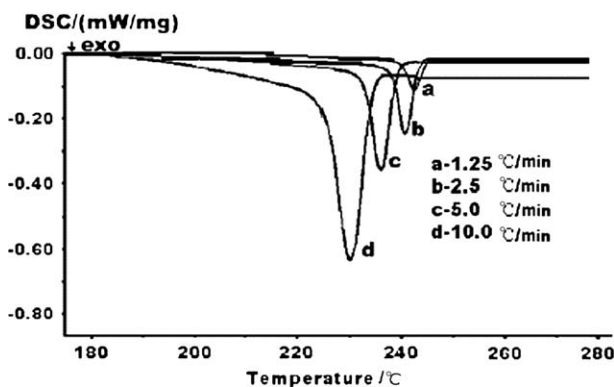


Fig. 10. DSC curves of 40 wt% n-HA/PA66 composites at different cooling rates.

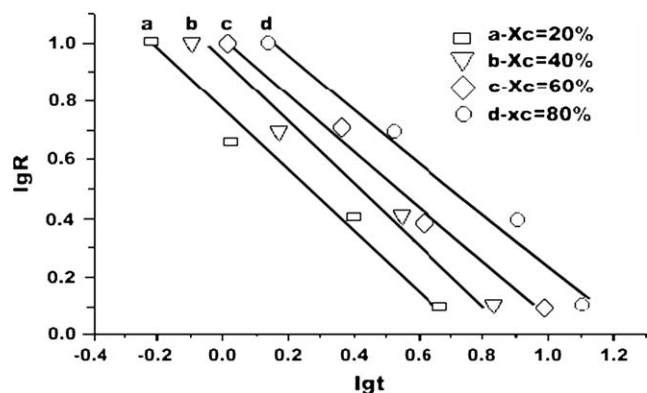


Fig. 11. Curves of  $\log R$  vs.  $\log t$  for different relative crystallization degree for 30 wt% n-HA/PA66 composite.

PA66 and n-HA/PA66 biocomposites with reference to n-HA content. It was found that n-HA/PA66 composites degraded later than did pure PA66. Furthermore, it was observed that the thermal stability of the n-HA/PA66 composites was higher than that of PA66, which is due to the hydrogen bonds between the amide group ( $-\text{NH}-\text{C}=\text{O}$ ) of PA66 and hydroxyl group ( $-\text{OH}$ ) of n-HA. DSC investigations showed that the incorporation of n-HA into PA66 caused an apparent increase in the  $T_c$ , however, a decrease in the percentage of crystallinity. These effects can be attributed to the fact that the hydroxyl groups on the surface of n-HA act as nuclei for the crystallization of the polymer. A model developed by Liu et al. was successful in describing the non-isothermal crystallization of PA66 and n-HA/PA66. The values of  $a$  for PA66 and n-HA/PA66 composites varied slightly, but the values of  $K_{(T)}$  systematically increased with increase of relative degree of crystallinity. For a certain relative degree of crystallinity, the value of  $K_{(T)}$  for n-HA/PA66 was smaller than that for PA66. That is, amounting to same relative degree of crystallinity, n-HA/PA66 required smaller

cooling rate, which indicated that n-HA/PA66 crystallizes at a quicker rate than PA66.

### Acknowledgement

This work was supported by the National “863” International Cooperation Program Foundation of China under grant No. 2002AADF3201.

### References

- [1] Bonfield W, Grynypas MD, Tully AE, Bowman J, Abram J. *Biomaterials* 1981;2:185.
- [2] Wang M, Bonfield W, Hench LL. *Bioceramics* 1995;8:383.
- [3] Wang M, Kokubo T, Bonfield W. *Bioceramics* 1996;9:387.
- [4] Chua B, Wang M. Hydroxyapatite reinforced polysulfone composites for potential medical applications. *Materials research society symposium proceedings 599: Mineralization in natural and synthetic biomaterials*. Boston, MA, USA; 1999. pp. 45–50.
- [5] Abu Bakar MM, Cheang P, Khor KA. *J Mater Process Technol* 1999;89–90:462.
- [6] Wang M, Weng J, Goh CH, Ni J, Wang CX. *Bioceramics* 2000;13:741.
- [7] Sousa RA, Reis RL, Cunha AM, Bevis MJ. *Bioceramics* 2000;13:669.
- [8] Ladizesky NH, Pirhonen EM, Appleyard DB, Ward IM, Bonfield W. *Compos Sci Technol* 1998;58:419.
- [9] Wang Xuejiang, Li Yubao, Wei Jie, de Groot Klass. *Biomaterials* 2002;23:4787.
- [10] Jie Wei, Yubao Li, Weiqun Chen, Yi Zuo. *J Mater Sci* 2003;38:3303.
- [11] Jie Wei, Yubao Li. *Eur Polym J* 2004;40:509.
- [12] Verheyen CCPM, de Wijn JK, van Blitterswijk CA. *J Biomed Mater Res* 1992;26:1277.
- [13] Peppas NA, Langer R. *Science* 1994;263:1715.
- [14] Damien CJ, Parson JR. *Appl Biomater* 1992;2:187.
- [15] McNeill C. In: Allen G, editor. *Comprehensive polymer science*, vol. 5. New York: Pergamon Press; 1989 [chapter 15].
- [16] Qin Huaili, Su Quansheng, Zhang Shimin, et al. *Polymer* 2003;44:7533.
- [17] Pramoda KP, Liu Tianxi, Liu Zhehui, He Chaobin, Sue Hung-Jue. *Polym Degrad Stab* 2003;81:47.
- [18] Davis Rick D, Gilman Jeffery W, Vander Hart David L. *Polym Degrad Stab* 2003;79:111.
- [19] Heughebaert M, LeGeros RZ, Gineste M, Guilhem A, Bone G. *J Biomed Mater Res* 1998;22:254.
- [20] Brill RJ. *Prakt Chem* 1942;161(2):49.
- [21] Howard W, Starkweather JR, Glover A, et al. *J Polym Sci: Polym Phys Ed* 1981;3:467.
- [22] Khanna YP, Kumar R, Reimschuessel AC. *Polym Eng Sci* 1988;28(24):1607.
- [23] Khanna YP, Reimschuessel AC, Banerjee A, Altman C. *Polym Eng Sci* 1988;28(24):1600.
- [24] Khanna YP, Kumar R, Reimschuessel AC. *Polym Eng Sci* 1988;28(24):1612.
- [25] Khanna YP. *Polym Eng Sci* 1990;30(24):1615.
- [26] Aharoni SM. *n-Nylons, their synthesis, structure, and property*. Chichester, New York: Wiley; 1997.
- [27] Avrami MJ. *Chem Phys* 1941;9:177.
- [28] Patel RM, Spruiell LJE. *Polym Eng Sci* 1991;31(10):730.
- [29] Ozawa T. *Polymer* 1971;12:150.
- [30] Liu TX, Mo ZS, Wang SE, Zhang HF. *Polym Eng Sci* 1997;37:568.

Table 3

Values of non-isothermal crystallization kinetic parameters for PA66 and n-HA/PA66 composites

	$X_c\%$	$F_{(T)}$	$a$
PA66	20	12.6	1.1
	40	15.5	1.1
	60	18.6	1.2
	80	22.9	1.2
30 wt% n-HA/PA66	20	6.0	1.1
	40	8.7	1.1
	60	10.5	1.0
	80	15.5	1.0
40 wt% n-HA/PA66	20	3.80	1.19
	40	6.03	1.21
	60	8.71	1.18
	80	13.48	1.18